クラスター構造の多様性と核反応によるアクセス

Makoto Ito[1,2] and K. Ikeda[2,3]

[1]Department of Pure and Applied Physics, Kansai University

[2]Rsearch Center of Nuclear Physics, Osaka University

[3]RIKEN Nishina Center for Accelerator based Science, RIKEN

内容

A. 構造・反応の統一研究の現状と今後

B. 天体核反応研究へ向けて：GCM + ABC法の応用

全体の構成

A. 構造・反応の統一研究の現状と今後

1. 軽核における化学結合様クラスター構造の研究

2. 反応によるクラスター状態へのアクセス

3. 研究の現状と今後の展開

B. 天体核反応研究へ向けて：GCM + ABC法の応用

1. 天体核反応と微視的クラスター模型

2. ABC法に関する最近の研究

3. ^{19}Ne = α + ^{15}Oクラスター状態とα共鳴散乱の研究

軽核における化学結合様クラスター構造の研究

1. 研究の背景：分子軌道描像によるこれまでの研究
2. 研究の目的：構造転移問題と分子軌道の拡張
3. 理論模型：一般化二中心クラスター模型
4. 計算と分析結果：偶Be同位体、^{10}C、^{18}O (現在進行中)

Cluster structures in 4N nuclei

IKEDA Diagram

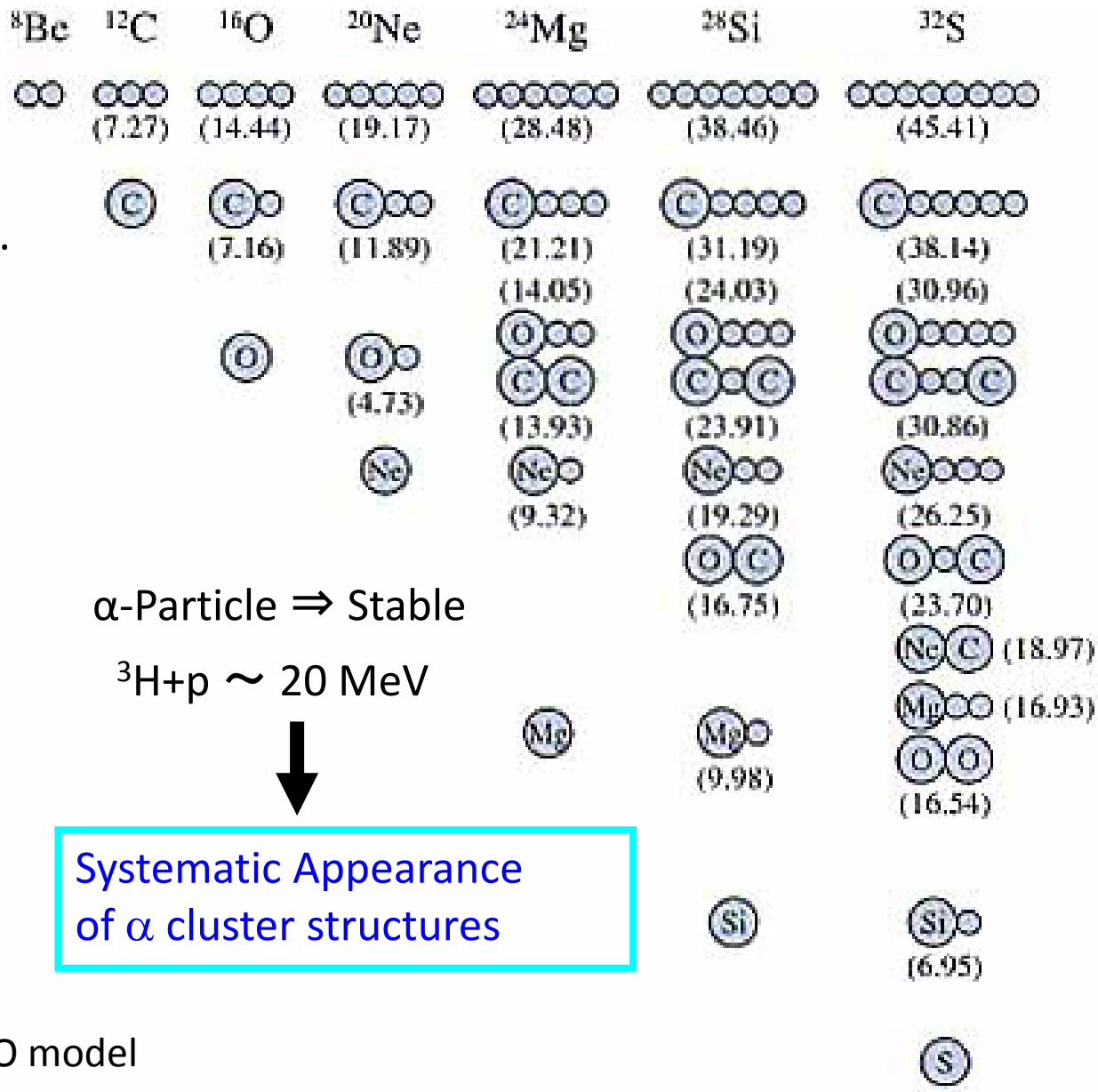

[Ikeda's Threshold rules]

Molecular structures will appear close to the respective cluster threshold.

Be isotopes

Molecular Orbital (MO) picture

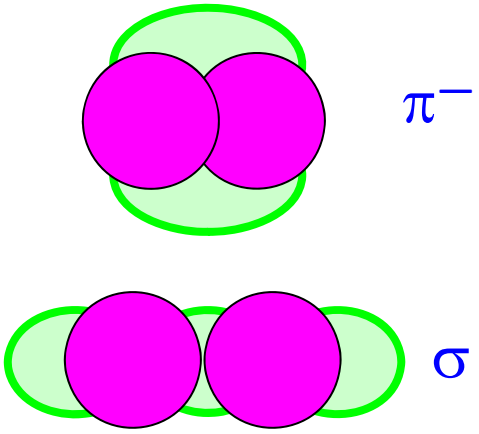

α-Particle ⇒ Stable

^{3}H+p ~ 20 MeV

Systematic Appearance of α cluster structures

There is a long history in the MO model

History of the MO models (1960s～)

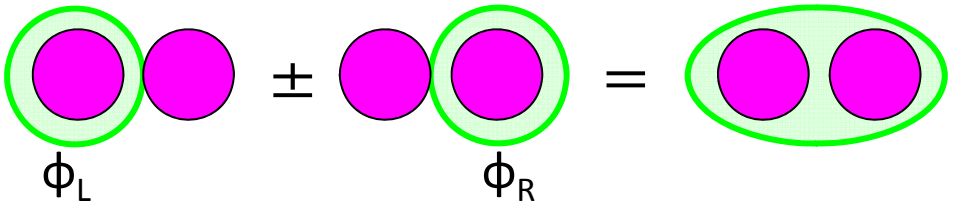

A. Pioneering works (1970s～)

1. Nucleon's exchange effect in the light-ion scattering, W. von Oertzen, NPA148 (1970)
2. Application of the MO model to N=Z systems, Y. Abe et al., PTP49 (1973)

B. Realistic applications (1980s～)

1. Systematic studies of binding mechanism in Be and B, M. Seya et al., PTP65 (1981)
2. Interpretation of the rotational bands in Be and B, W. von Oertzen , ZPA354 (1996)
3. Transfer reactions in $^{12}C+^{13}C$, $^{16}O+^{17}O$ etc., B. Imanishi et al. , Phys. Rep. 155 (1987)

C. Study of ^{10,12}Be by the revised MO model (1996～)

1. Improvement of the covalent orbits, N. Itagaki et al., PRC61 (2000)
2. Molecular pictures in Be isotopes, Y. Kanada-Enyo et al. , PRC66 (2002)

D. Extension of the MO model (in progress)

1. Ne isotopes ($\alpha+^{16}O+N+N+\ldots$), M. Kimura, PRC75 (2007)
2. C isotopes ($3\alpha+N+N+\ldots$), N. Itagaki et al., PRC74 (2006)

MO picture gives one of the general and standard pictures in nuclear clustering phenomena

Beyond the MO picture in unbound states (2004 ～)

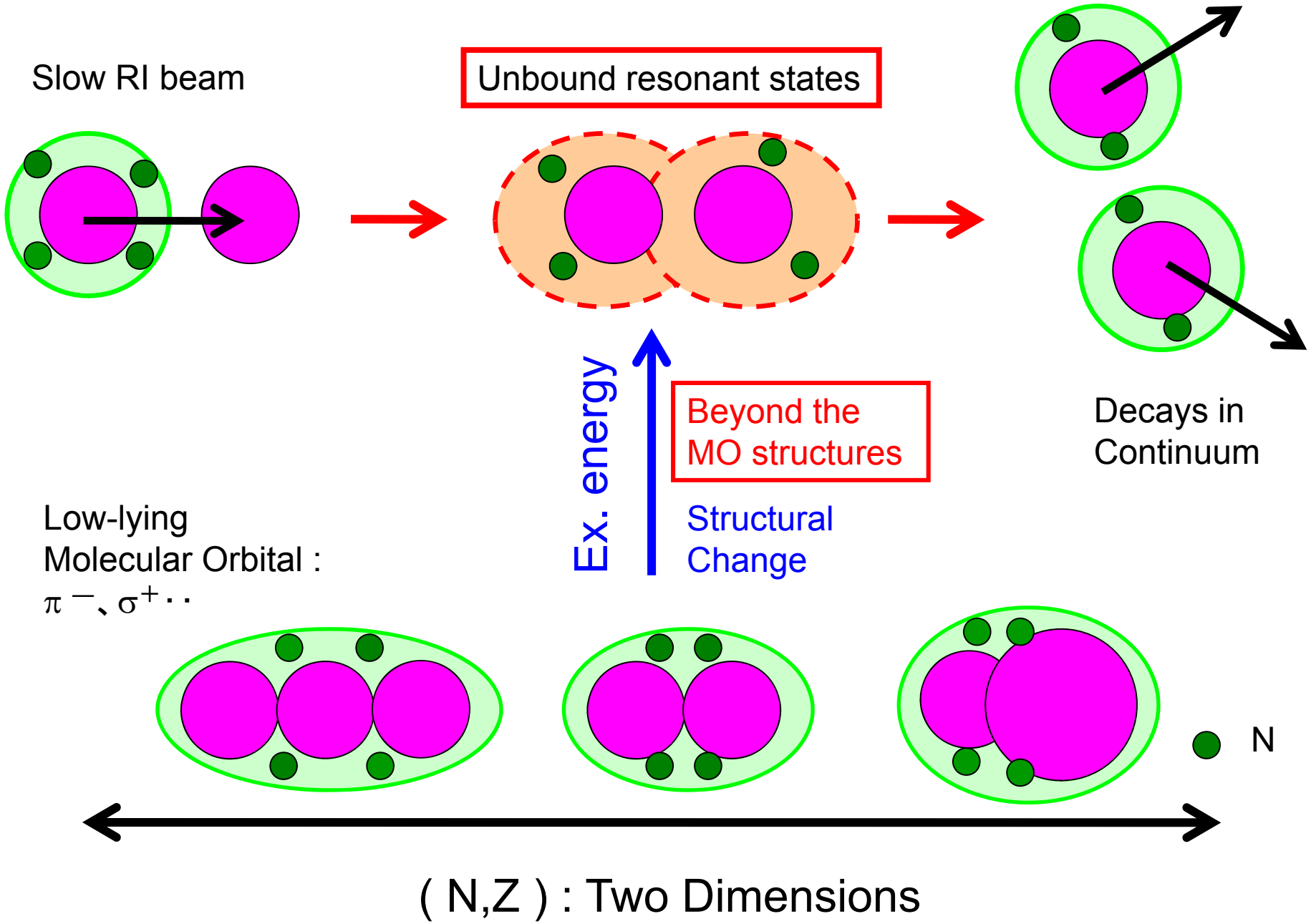

MO modelの拡張

低励起～高励起状態を包括した構造転移の追跡は、核多体系を深く理解する上で必須である

分子軌道模型を拡張することが重要!

我々の模型 (^{12}Be=α+α+4N)

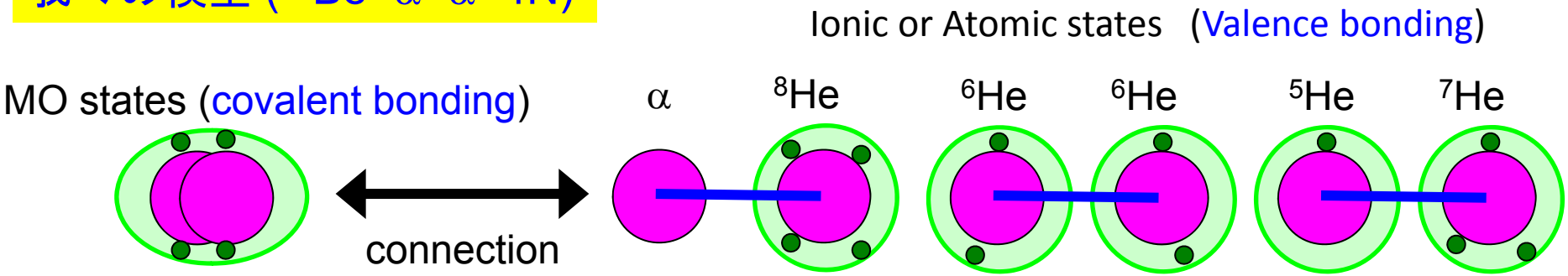

Unified model of covalent, atomic, ionic configurations

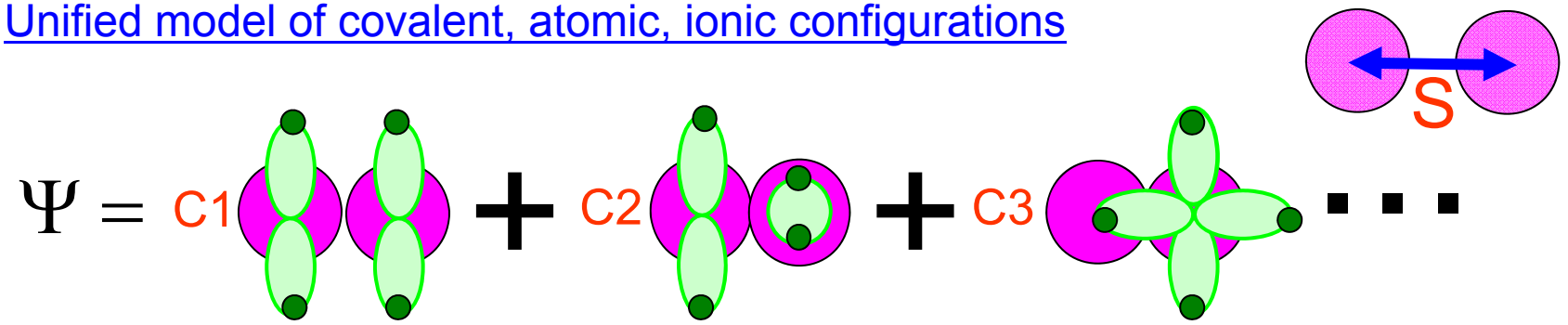

0Pi (i=x,y,z) Coupled channels of atomic orbits

S, Ci : Variational p.r.m.

M. Ito et al., PLB588 (2004), PLB636 (2006)

Formulation (I) : Extension of the MO model

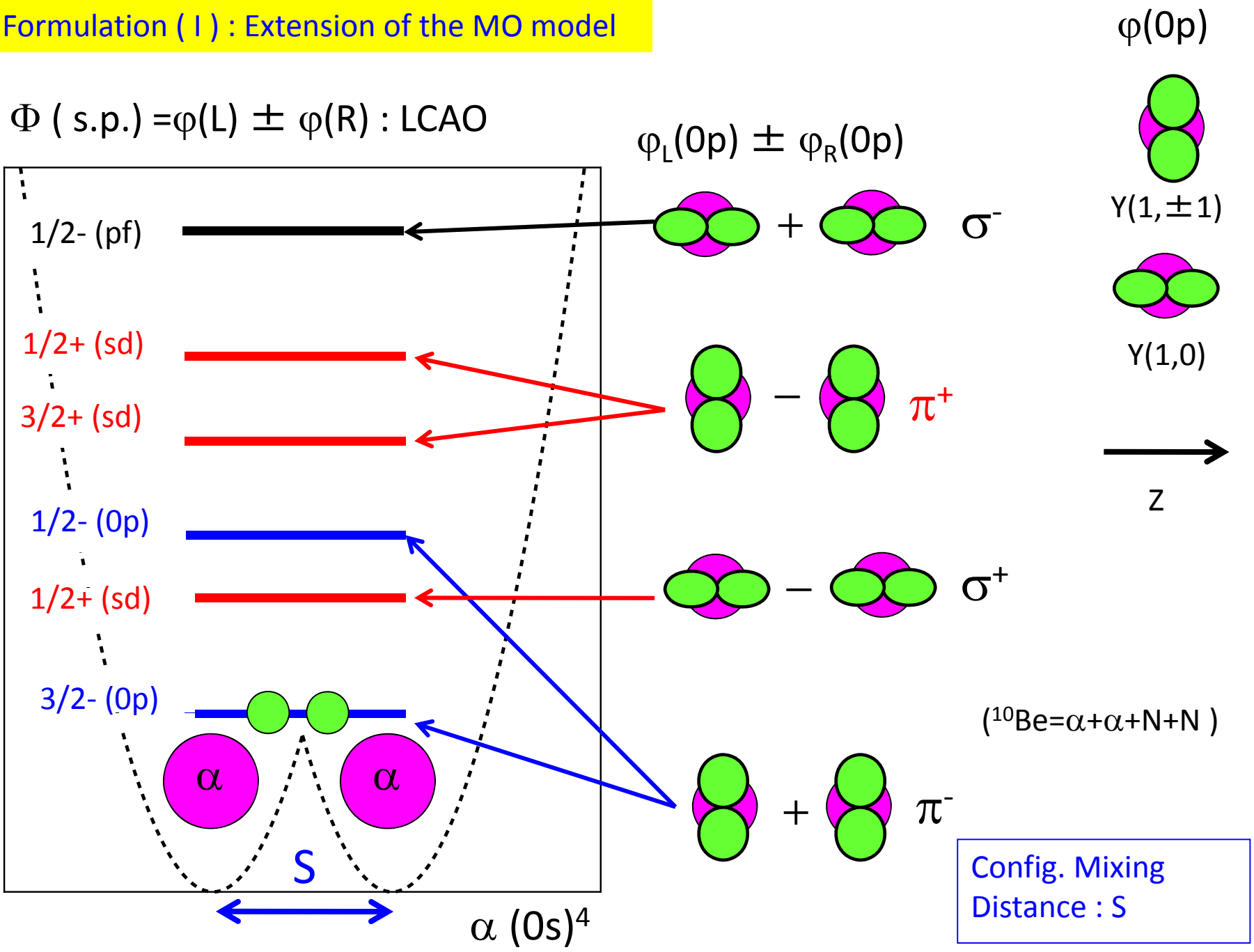

Formulation (II)

Linear Combination of Atomic Orbital (LCAO)

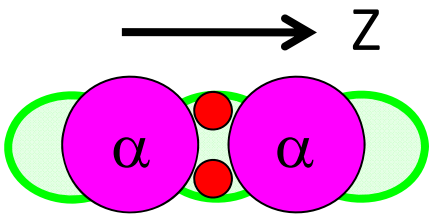

$$(\sigma^{+})^2 = \left(P_z(L) - P_z(R) \right)^2$$

$$= P_z(L)\cdot P_z(L) + P_z(R)\cdot P_z(R) - 2P_z(L)\cdot P_z(R)$$

$^6He + \alpha$ $\quad$ $\alpha + {}^6He$ $\quad$ $^5He + {}^5He$

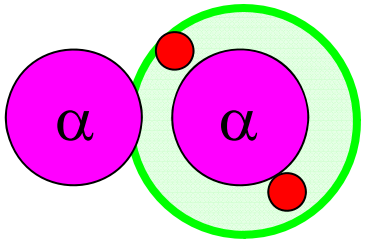

$\alpha + {}^6He(0^+)$

$$= P_x(R)\cdot P_x(R) + P_y(R)\cdot P_y(R) + P_z(R)\cdot P_z(R)$$

General MO: $\left(C(L)P_i(L) + C(R)P_j(R)\right)^2$

Total wave function

$$\Psi = \sum_{\beta,S} C(\beta,S)\, P_m(a)\cdot P_n(b)$$

Variational PRM

$(m,n)=x,y,z$ $\quad$ $(a,b) = L,R$

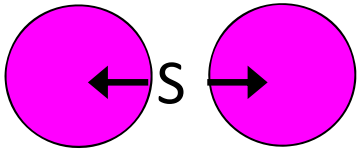

Generalized Two-center Cluster model

Basis function

$$\Phi^{J\pi}_{K}(\nu,S) = P^{J\pi}_{MK}\, A\, \{\, \phi_L(\alpha)\, \phi_R(\alpha)\, \chi(\nu)\, \}_S$$

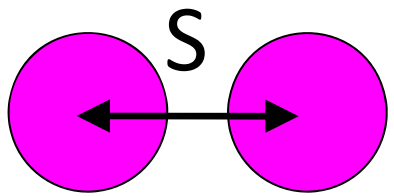

$\phi(\alpha)$: $(0s)^4$ in H.O.

$\chi(\nu)$: Neutrons (Left or Right, $0p_i$, i=x,y,z)

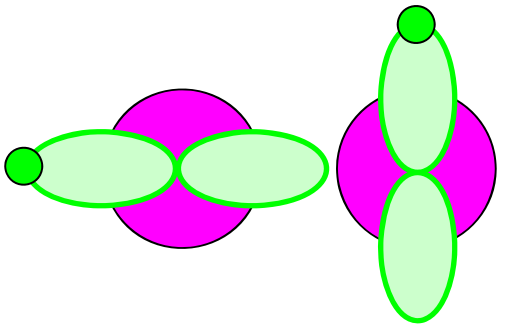

Eigenvalue equations

Total W.F. : $\Psi^{J\pi} = \Sigma_S \; \Sigma_\nu \, f(\nu,S)\, \Phi^{J\pi}_{K}(\nu,S)$

$< \Phi^{J\pi}_{K}(\nu,S') \mid H - E \mid \Psi^{J\pi} > = 0$ (Full GCM)

Fixed S → Adiabatic Energy surfaces

K-projection

1. Analytic K-projection

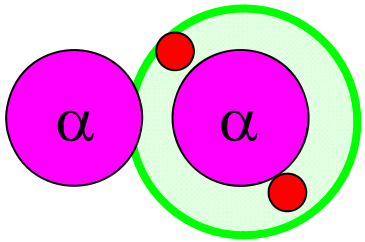

[α+^{6}He(I^{+})] K=0

K=0 basis　　K=0 basis

$0^{+} \rightarrow P_x(R)\cdot P_x(R) + P_y(R)\cdot P_y(R) + P_z(R)\cdot P_z(R)$

$2^{+} \rightarrow P_x(R)\cdot P_x(R) + P_y(R)\cdot P_y(R) - 2P_z(R)\cdot P_z(R)$

K (and I) projection is possible in an analytic way ⇒ very tedious for many nucleons

2. Numerical K-projection

K-projection is done by diagonalizing the J_z operator

$$J_z\,\Phi(K) = K\,\Phi(K) \qquad \Phi(K) = \sum_{\alpha} C_{\alpha}\,\varphi(\alpha)$$

Similar manner to the M-scheme in the shell model

$$J_z = \sum_{i=1}^{A} j_z(i)$$

Atomic orbit in the cartesian coordinate

Be isotopes from bounds to continuum : $J^{\pi} = 0^{+}$

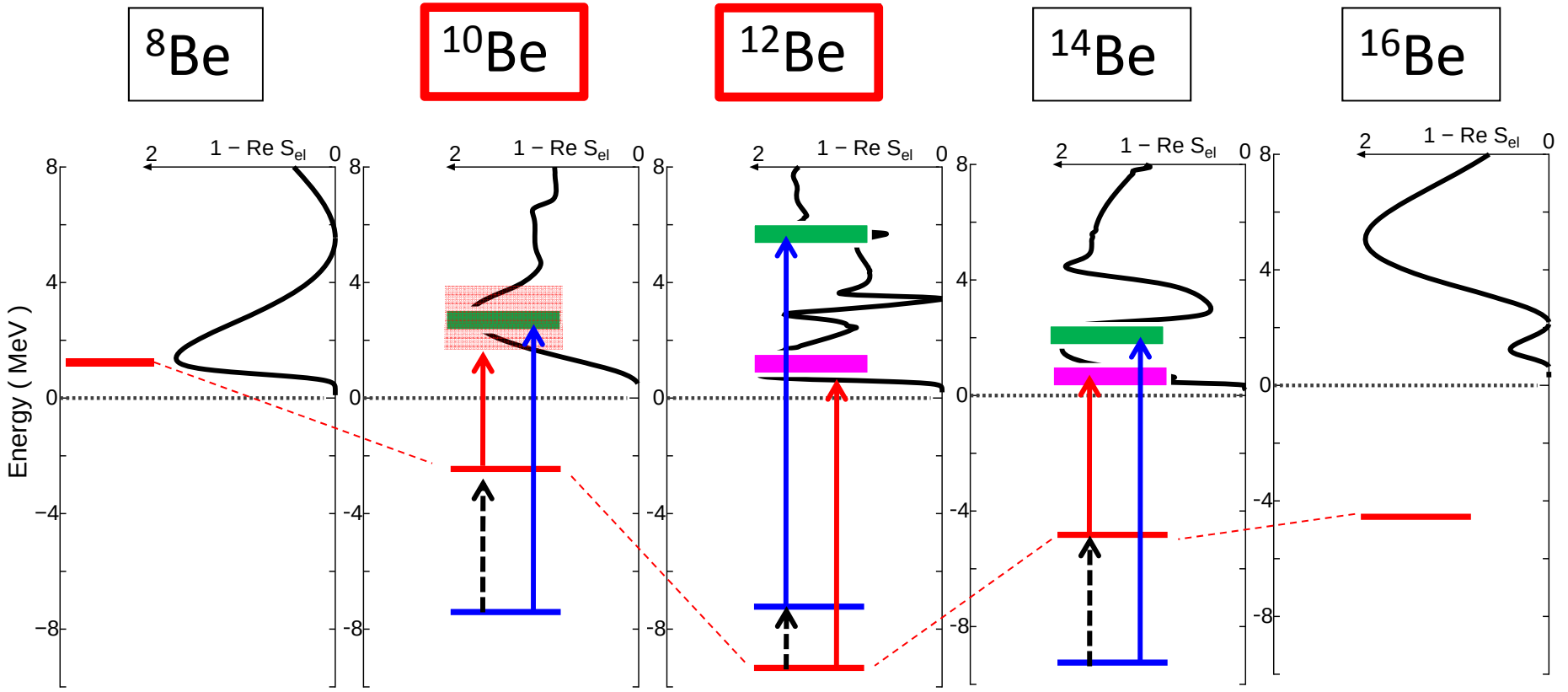

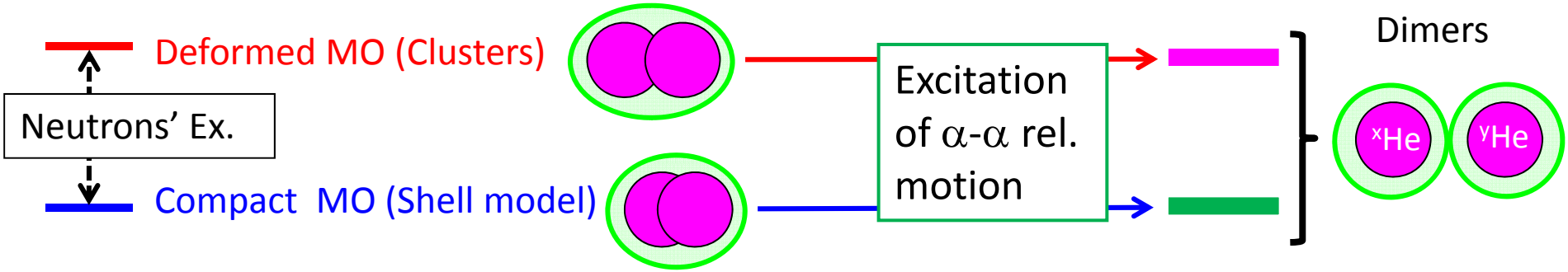

Classification of the excitation degrees of freedom in ^{10,12}Be

^{10}Be = α + α + 2N

^{12}Be = α + α + 4N

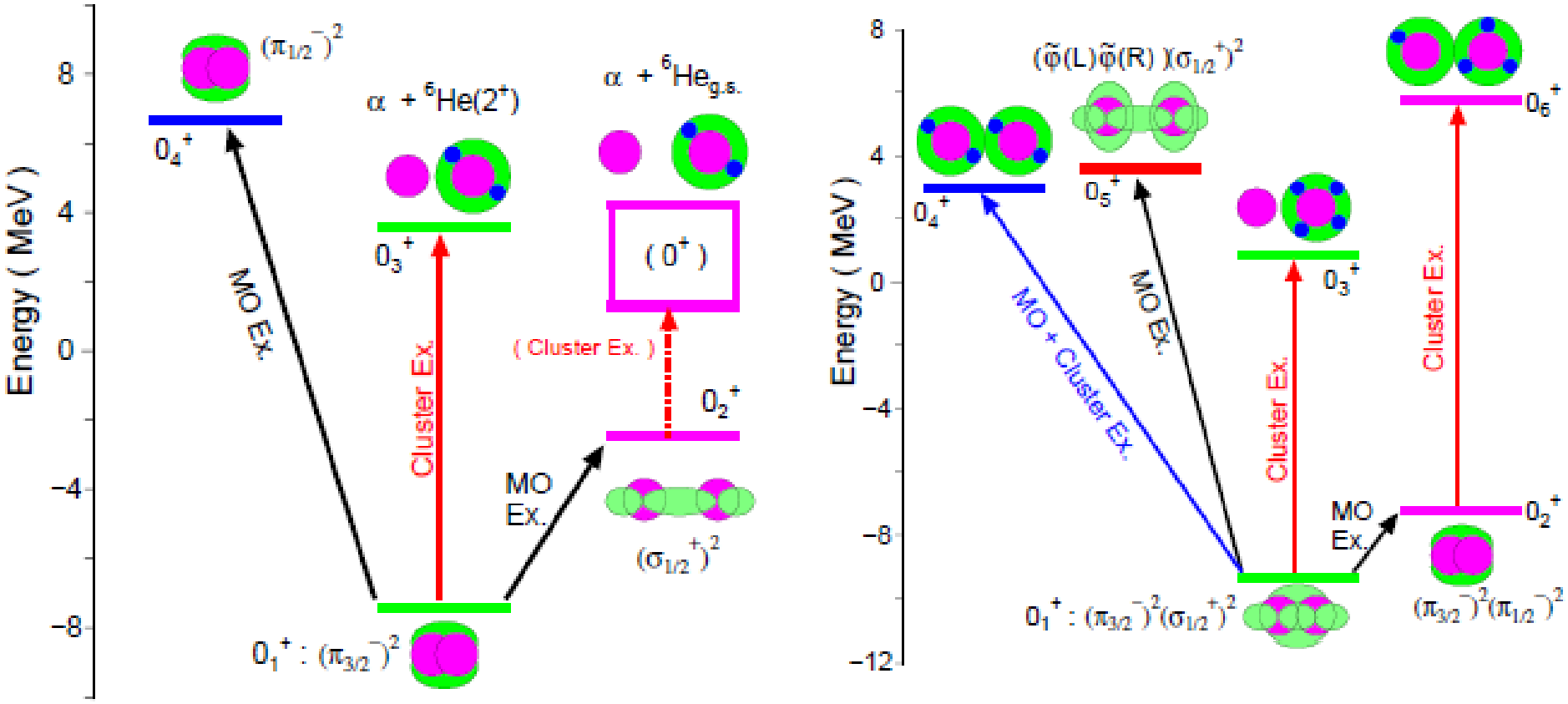

Double degrees of freedom (α cluster + neutrons) prominently appears in Be isotopes.

A candidate of the direct probe of the excited states is the monopole transition

Overlap Functions for the 0_1^+ and 0_3^+ states (Preliminary)

The 0_1^+ state (Deformed MO)

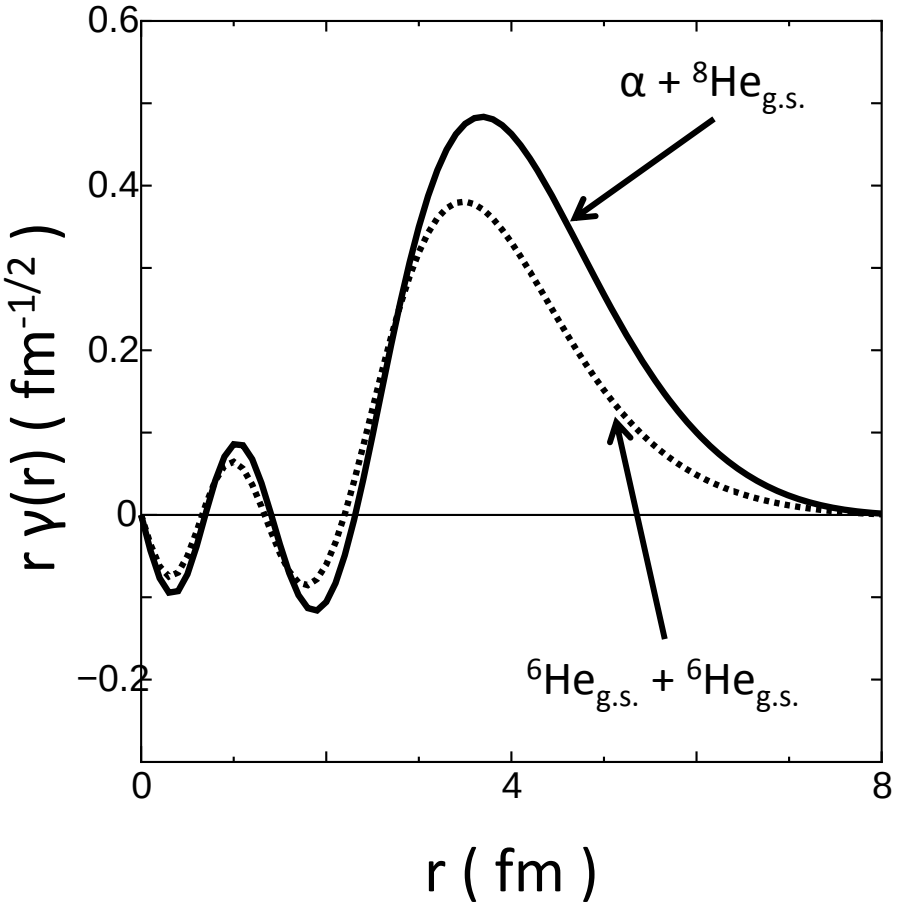

The 0_3^+ state (Developed $\alpha + {}^8\mathrm{He}_{g.s.}$)

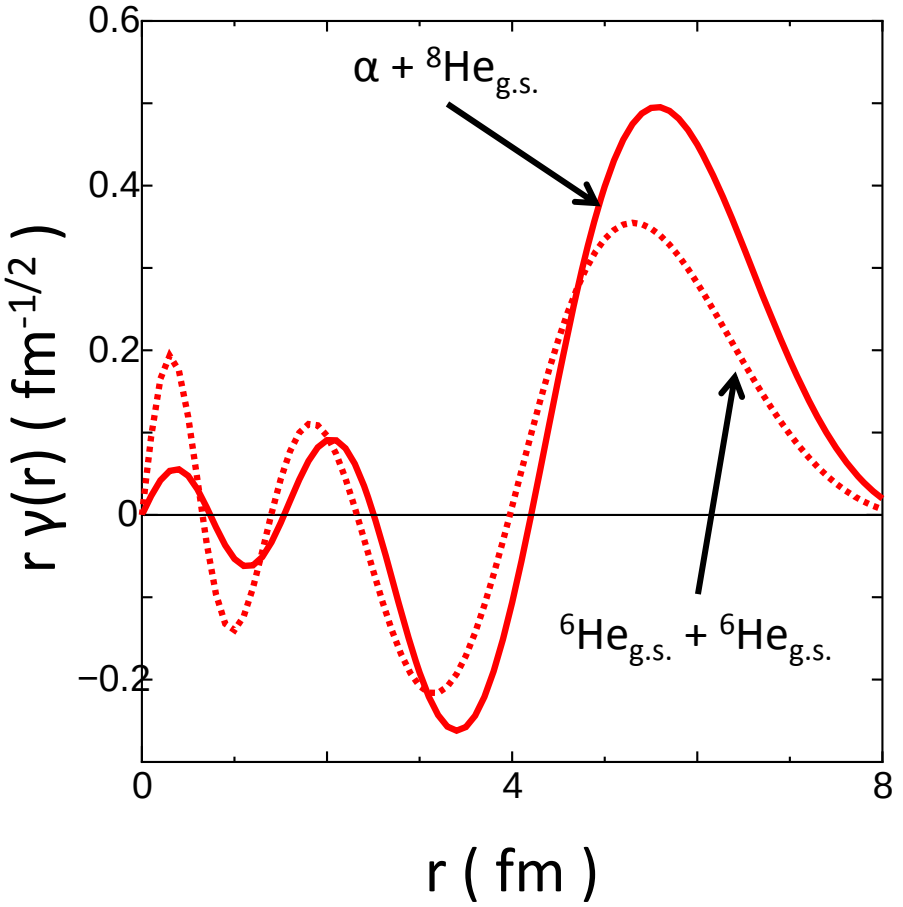

Radial excitation of the relative wave function occurs in $0_1^+ \Rightarrow 0_3^+$

Variety of Nuclear Chemical Clusters: Subject

Question

What is a variation in replacing α core or valence neutrons ?

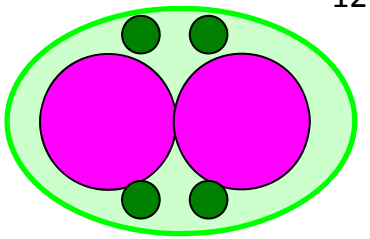

$^{12}Be = \alpha + \alpha + 4N$

Strongldegeneracy of chemical bonding states

+ 2N

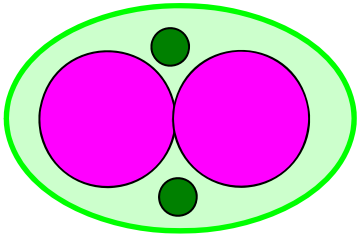

$^{10}Be = \alpha + \alpha + 2N$

2N ⇒ 2P

α ⇒ ^{12}C

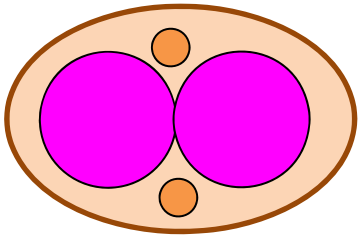

$^{10}C = \alpha + \alpha + 2P$

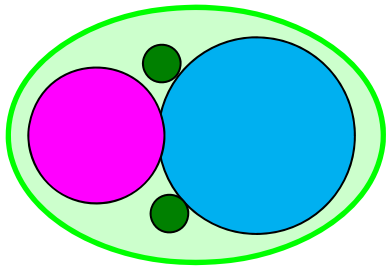

$^{18}O = \alpha + {}^{12}C + 2N$

^{10}Be and ^{10}C ($J^{\pi} = 0^{+}$)

Considerable Coulomb shift occurs only in the Non-S wave states ⇒ A kind of Thomas-Ehrman shift

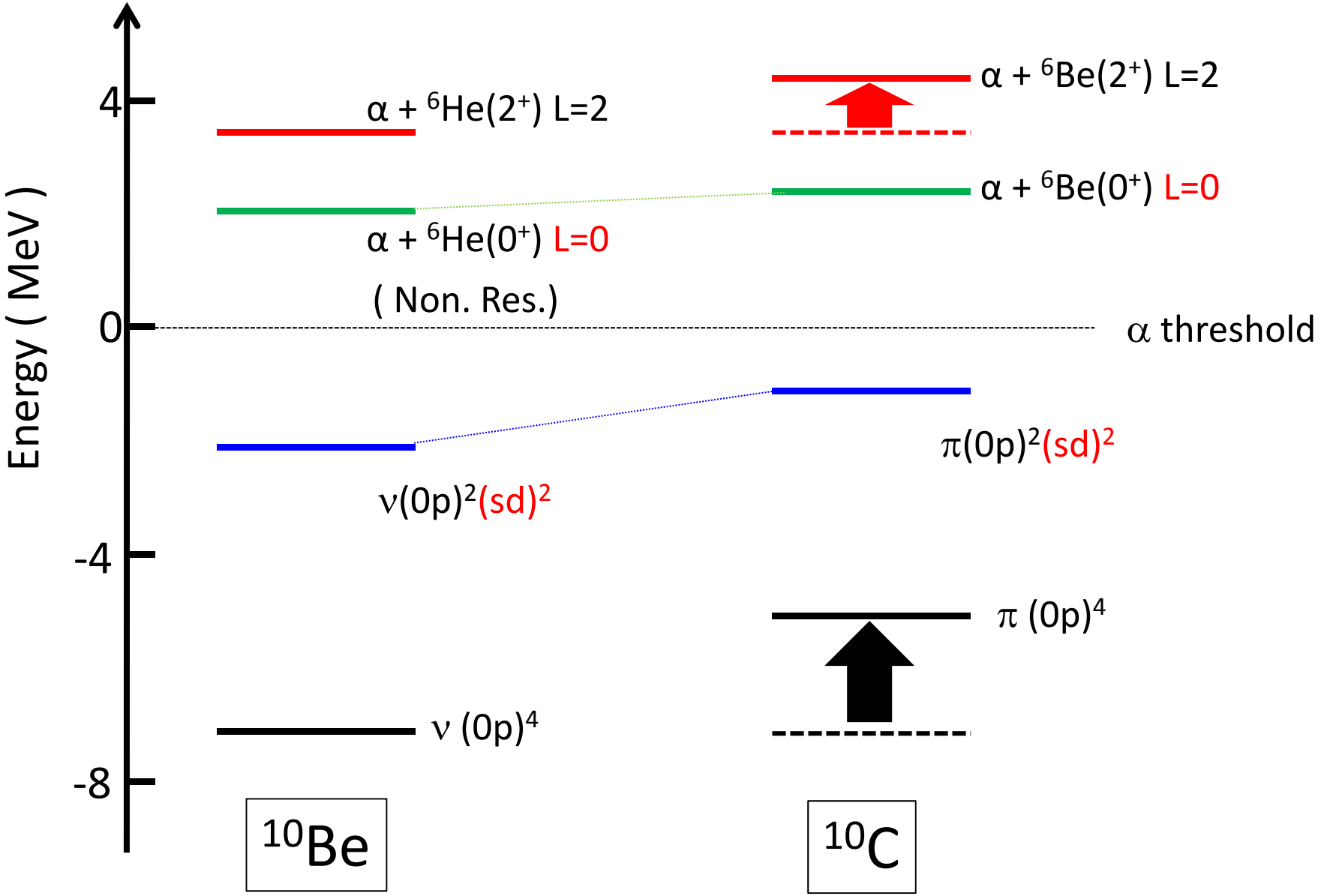

Comparison of ^{10}Be with ^{18}O (Theory)

Large Energy for a neutron excitation
⇒ Degeneracy of two levles

^{10}Be = (α+^{6}He) +(^{5}He+^{5}He)

^{18}O = (α+^{14}C) +(^{5}He+^{13}C)

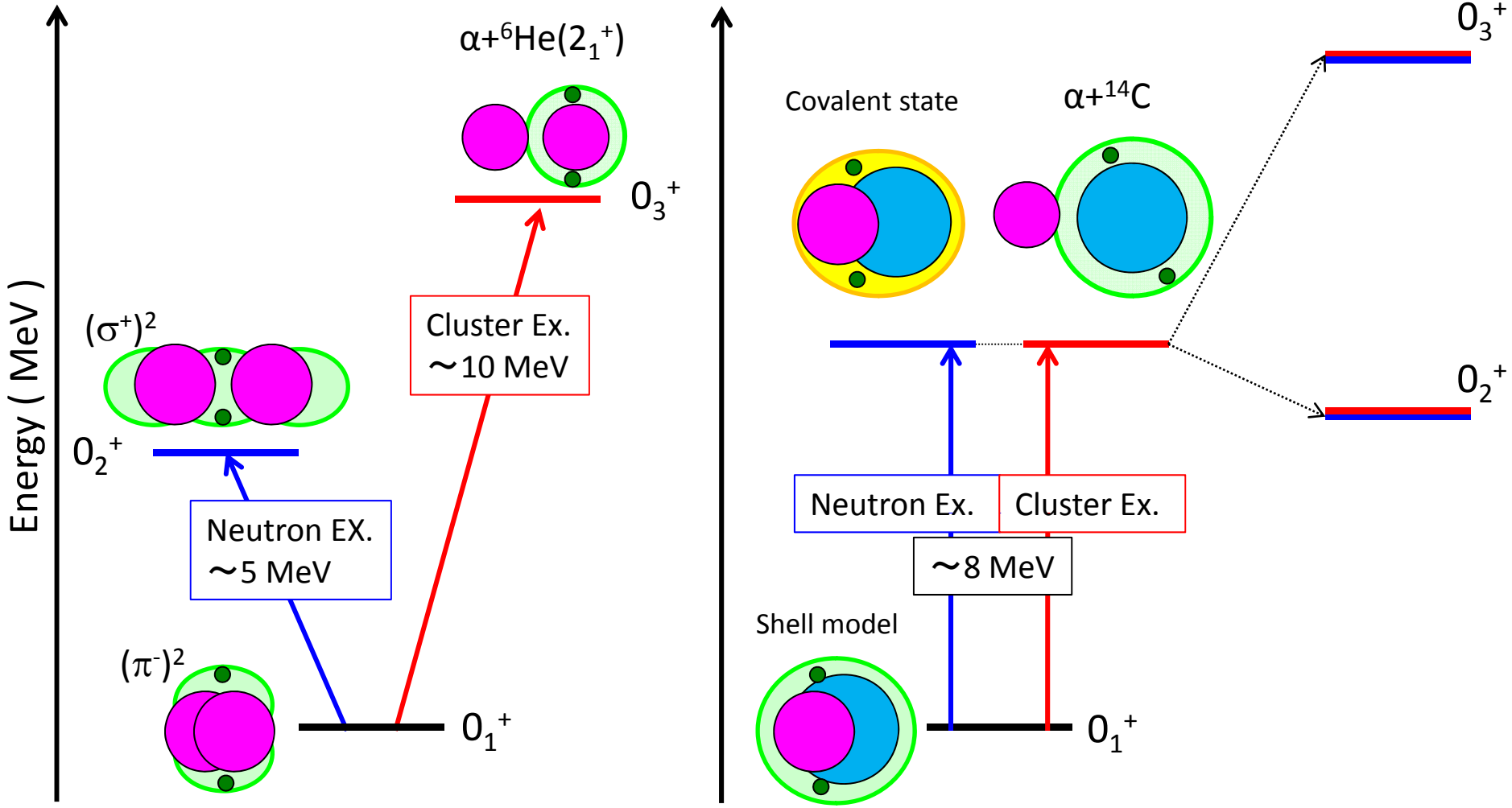

Coupling effect of neutron ex. and Cluster ex. is small.

Coupling effect of neutron ex. and Cluster ex. is Large.

Variety of “Nuclear Chemical Clusters” : Present results

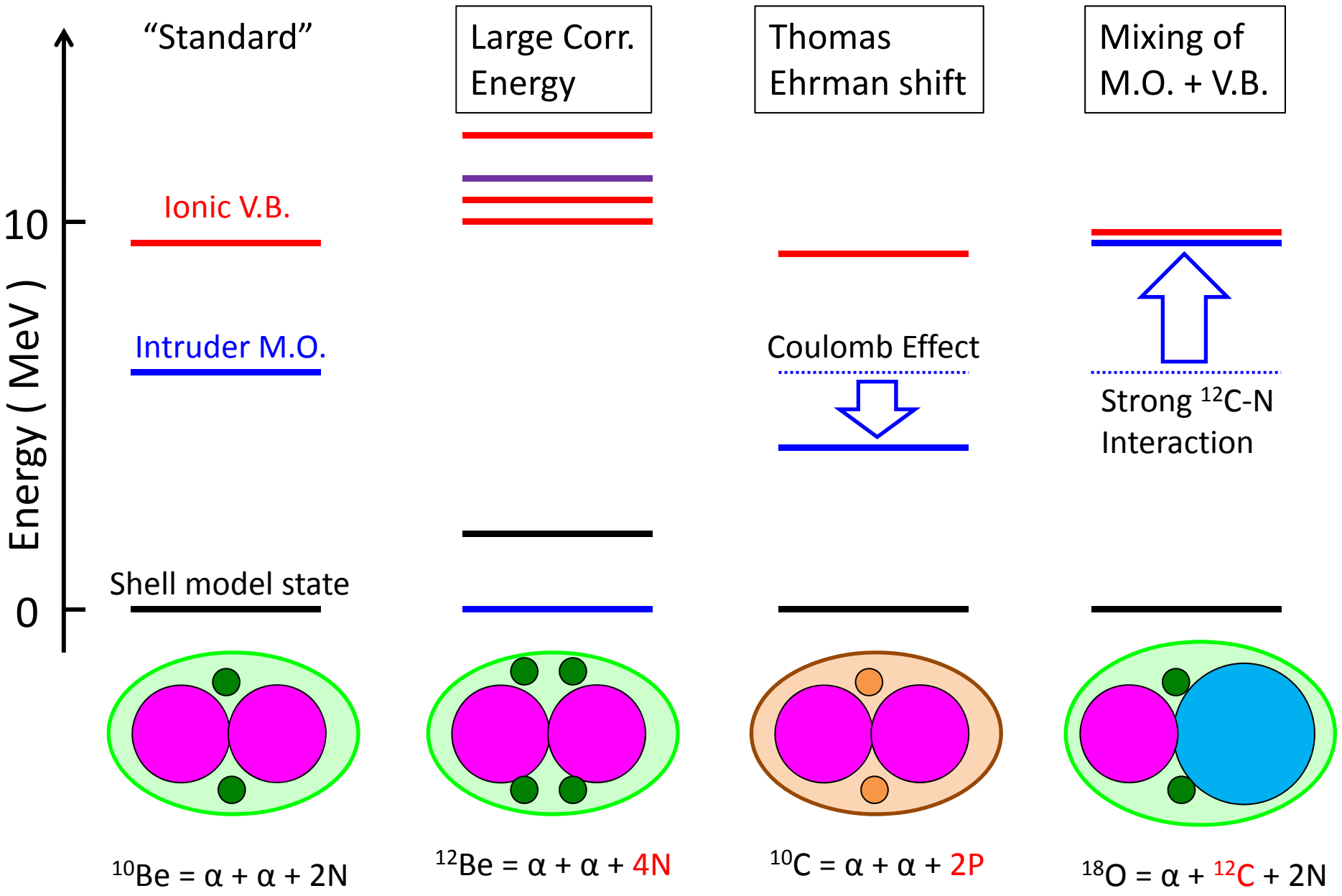

反応によるクラスター状態へのアクセス

1. 共鳴散乱によるクラスター状態励起

A. α + ^{8}He ⇒ ^{6}He + ^{6}He反応

B. α + ^{6}He非弾性散乱における非断熱遷移

2. モノポール遷移によるクラスター励起

A. ^{12}BeにおけるISとIVモノポール遷移

B. ^{10}Be－^{10}C：ISモノポール遷移と荷電対称性

3. 散乱半径法による反応分析

P + ^{12}Cによるクラスター励起と反応サイズ

1. 共鳴散乱によるクラスター状態励起

Coupling to open channels in continuum

M. Ito et al., PRL100 (2008), PRC81 (2011)

Closed states method : Prof. Kamimura, Prog. Part. Nucl. Phys. 51 (2003)

Open channels　　Compound states (Closed)

$$\Psi^{(+)} = \sum_{\beta} \varphi_{\beta} \chi^{(+)}_{\beta,\alpha} + \sum_{\nu} b_{\nu} \Omega^{K=0}_{\nu}$$

Bound state approximation with Atomic Orbital Basis

Scattering B.C.

$$(H - E_{\nu}) \Omega^{K=0}_{\nu} = 0$$

400～500 S.D. with J^{π} projection

$$\chi^{(+)}_{\beta,\alpha} \xrightarrow[R_{\beta}=\infty]{} u^{(-)}_{L_{\beta}} \delta_{\beta,\alpha} - S_{\beta,\alpha} u^{(+)}_{L_{\beta}}$$

Rearrangement channels : ^{12}Be = α + ^{8}He$_{g.s.}$、 ^{6}He$_{g.s.}$ + ^{6}He$_{g.s.}$、^{5}He$_{g.s.}$ + ^{7}He$_{g.s.}$

Calculation of the coupling of the open channel and closed compound states

Open channels　　Compound states (Closed)

$$\Psi_c^{(+)} = \sum_\beta \mathrm{A}\left\{\varphi_\beta \chi_{\beta,c}^{(+)}\right\} + \sum_\nu b_\nu \Omega_\nu^{K=0}$$

$$(H-E)\Psi^{(+)} = 0$$

$$\left\langle \Omega_\nu^{K=0} \middle| H \middle| \Omega_{\nu'}^{K=0} \right\rangle = \varepsilon_\nu \delta_{\nu,\nu'}$$

$$\chi_{\beta c}^{(+)}(R_\gamma) = \sum_{i=0}^{n} C_{\beta i}^{(c)} u_{\beta i}(R_\beta)$$

$$b_\nu = \frac{-1}{\varepsilon_\nu - E}\left\langle \Omega_\nu^{K=0} \middle| (H-E) \middle| \sum_\beta \mathrm{A}\left\{\varphi_\beta \chi_{\beta,c}^{(+)}\right\} \right\rangle$$

Closed states　　Open channels

(S.D. of the Brink w.f.)　　(S.D. of the Brink w.f.)

⇩

Closed states can be replaced to the more sophisticated states like AMD.

Cross sections of neutron transfers

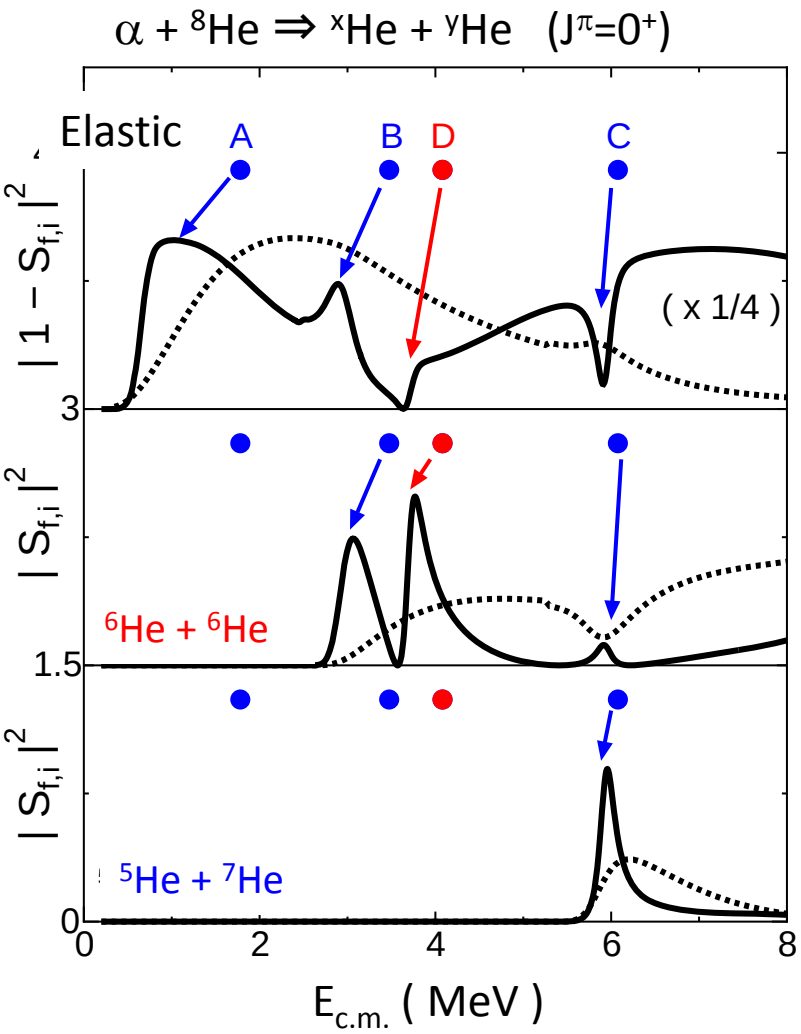

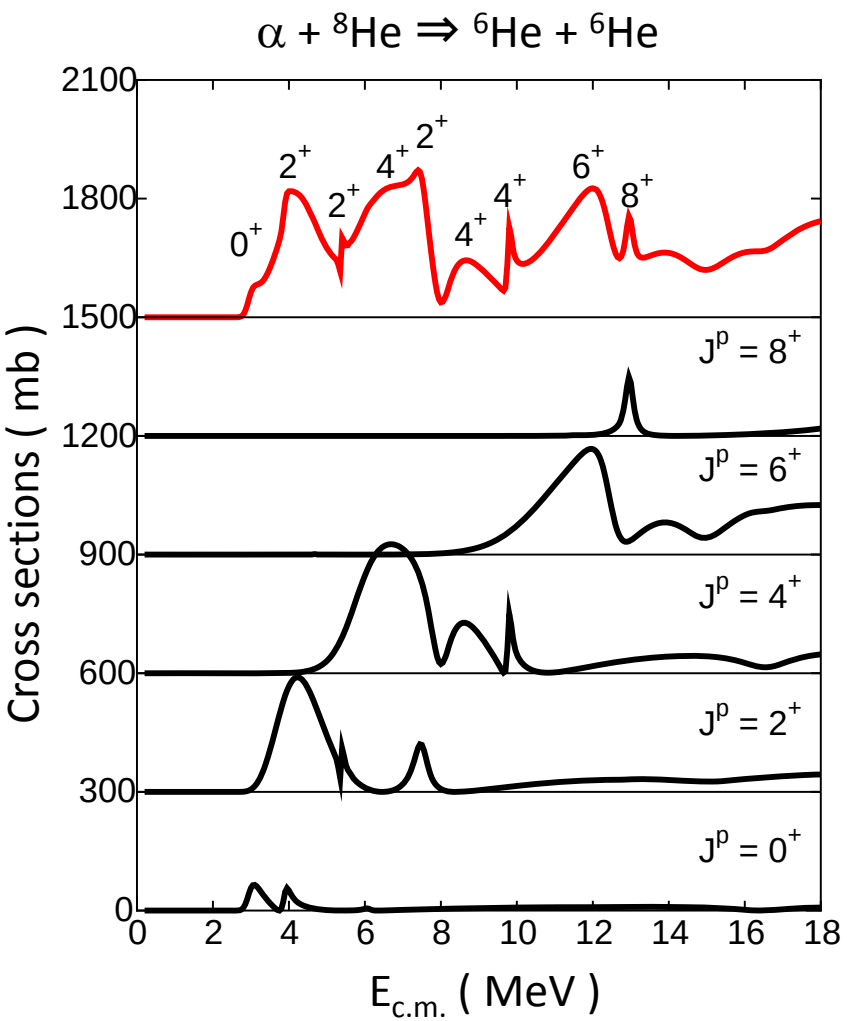

Dotted curves : Three open channels only

Solid curves: Open + closed chanels

This is a prediction for recent experiments at GANIL.

Enhancement of the two neutron transfer

$$\left|\Phi\,(Cov.SD)\right\rangle = \left|\chi(^6He+^6He)\right\rangle + \left|\varphi(^5He+^7He)\right\rangle$$

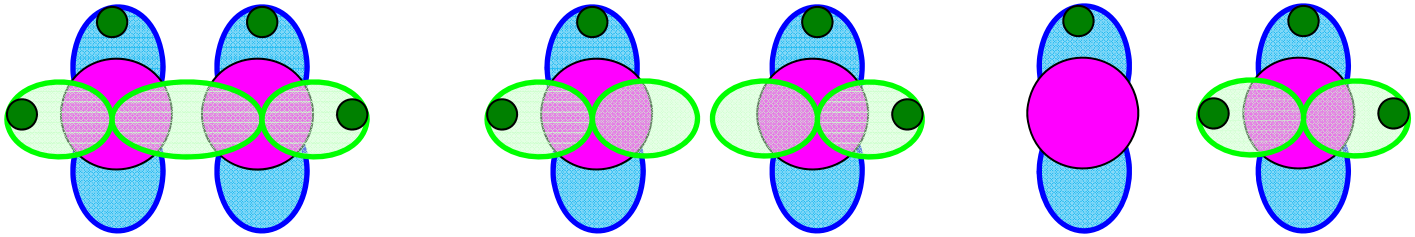

Open

Closed

Strong decay into ^{6}He+^{6}He

Covalent SD, $|S_{f,i}|^2=1$

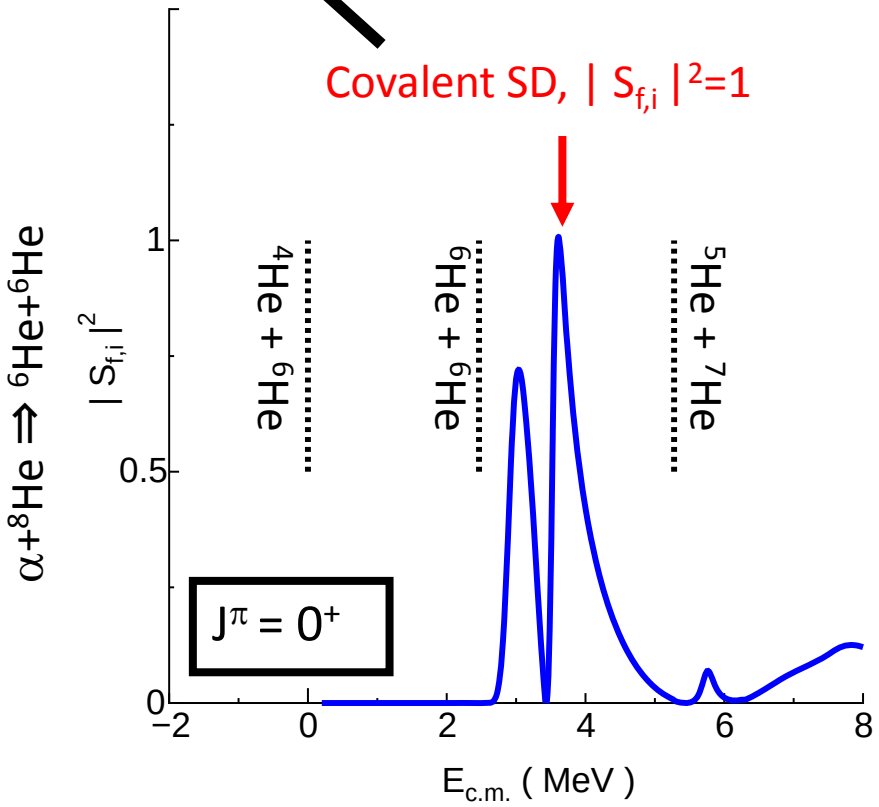

S-matrix reaches almost unity.

$$\left|S\left(^6He+^6He \leftarrow \alpha+^8He\right)\right|^2 \approx 1$$

Large part of the flux flows to ^{6}He+^{6}He.

Consistent to Exp. of ^{12}Be breakup
By S. Shimoura et al.

E_x spectra of ^{12}Be(α,α′)^{4}He^{8}He (positive parities)

- E_x spectra of pos.-parity states
- Fitting with resonances determined in ^{6}He+^{6}He analysis (E_R & Γ_R: fixed for J=0 & 2)

–10 MeV: Korsheninnikov et al., PLB343('95)53.

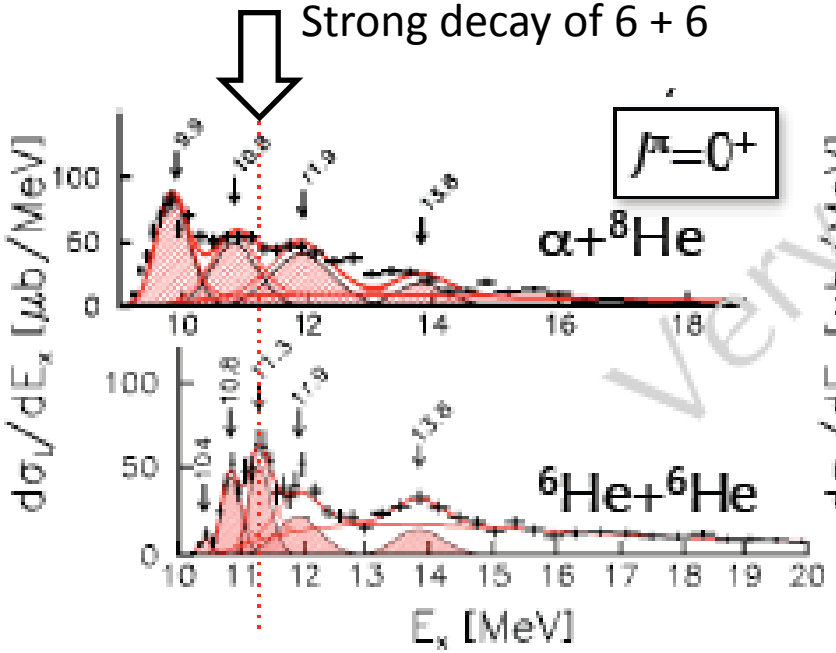

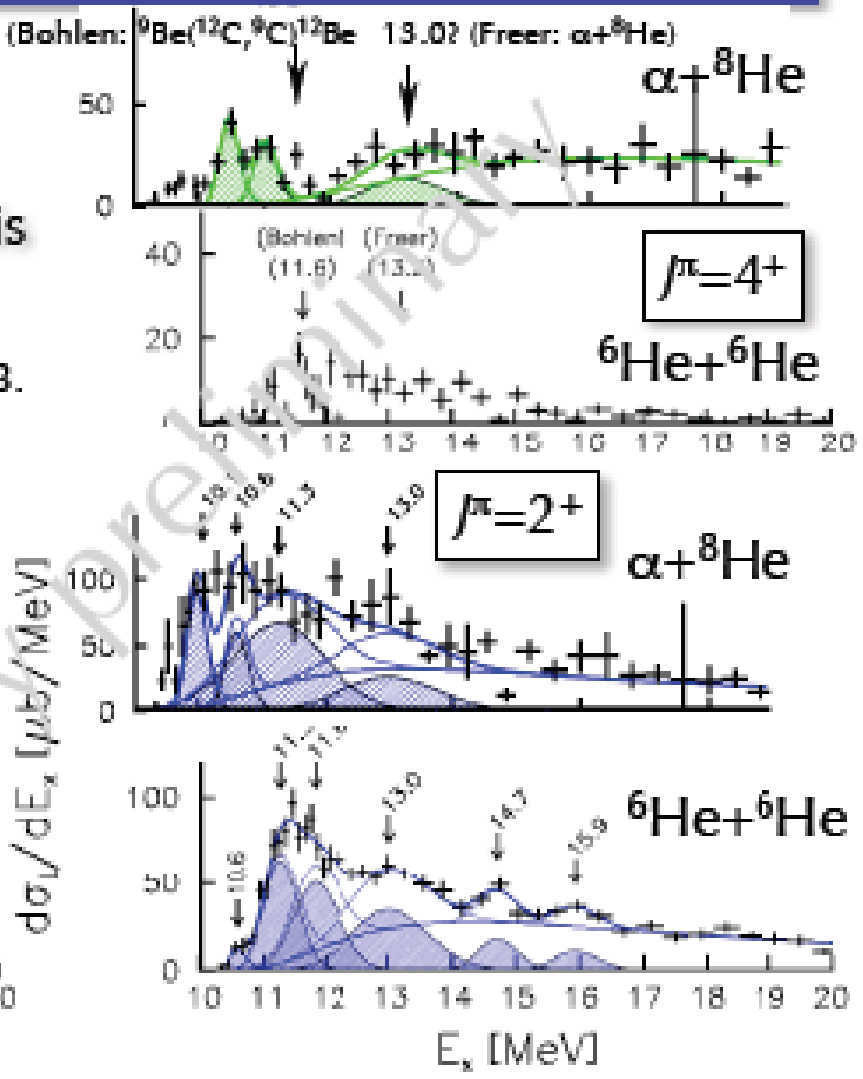

Extraction of the $J^{\pi}=0^{+}$ strength in $\alpha+^{8}He \Rightarrow {}^{6}He+{}^{6}He$

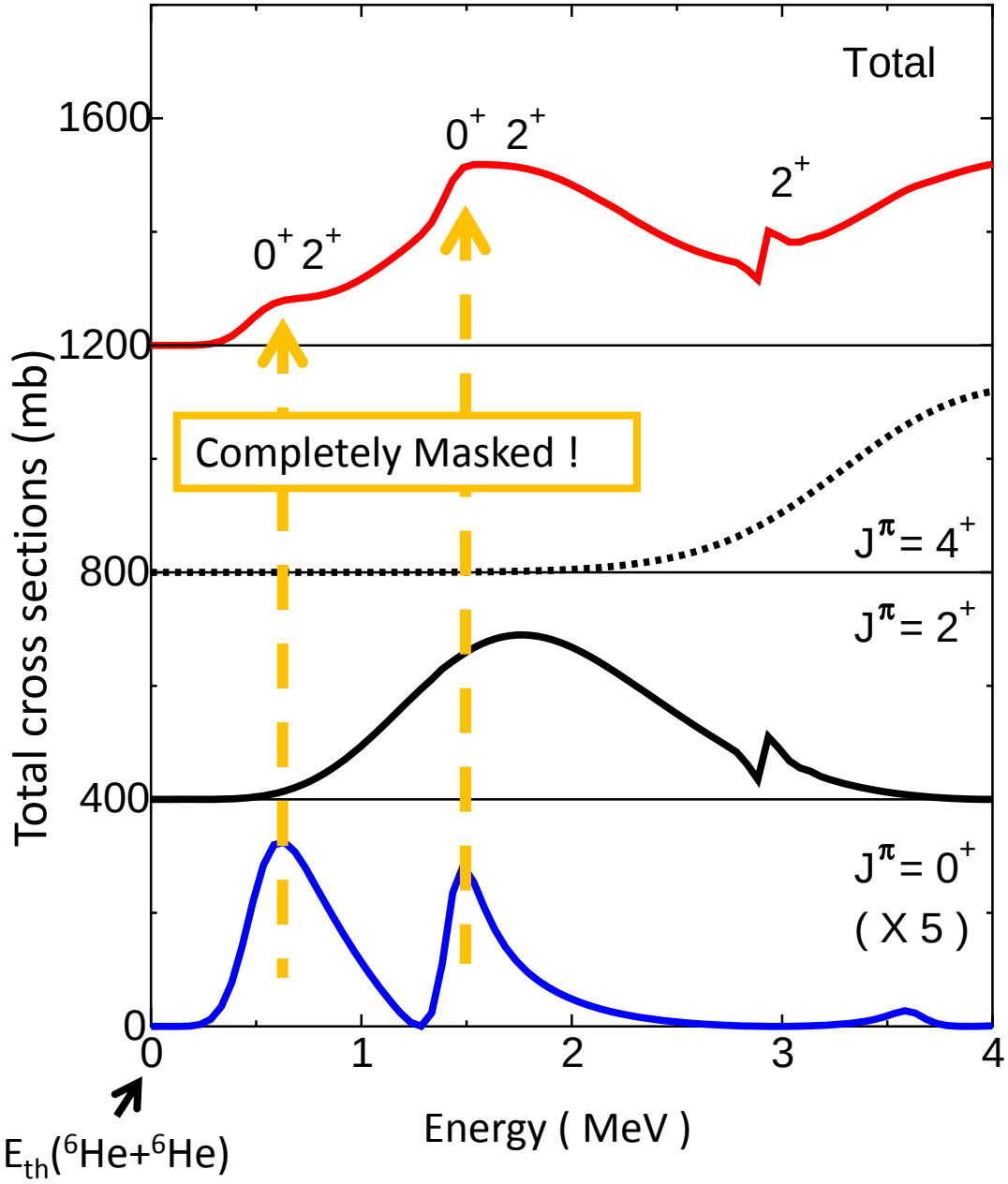

Precise measurements of scattering will be available !

$$\sigma(E) = \frac{\pi}{k^2} \sum_{J=even} (2J+1) \left| S^{J}_{f,i}(E) \right|^2$$

The $J^{\pi}=0^{+}$ strength is quite small .

(Due to a factor of 2J+1)

$J^{\pi}=2^{+}$ strength is dominant.

(4^{+} strength is negligible.)

We should extract the 0^{+} contribution from the total strength.

Angular distributions for the resonances of α+^{8}He ⇒ ^{6}He+^{6}He

$$\frac{d\sigma}{d\Omega} = \frac{1}{4k^2}\left|\sum_{J=0,2}(2J+1)\,S_{f,i}(J,E)\,P_J(\cos\vartheta)\right|^2$$ For Spinless channels

Lower Resonance (^{6}He+^{6}He)

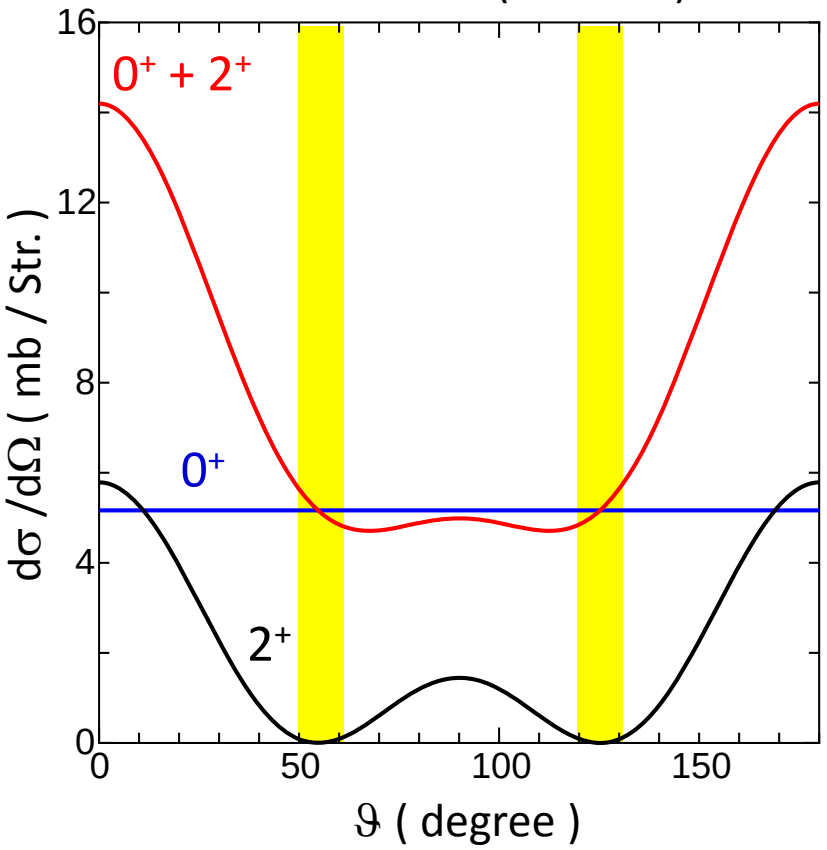

Higher Resonance (Covalent SD)

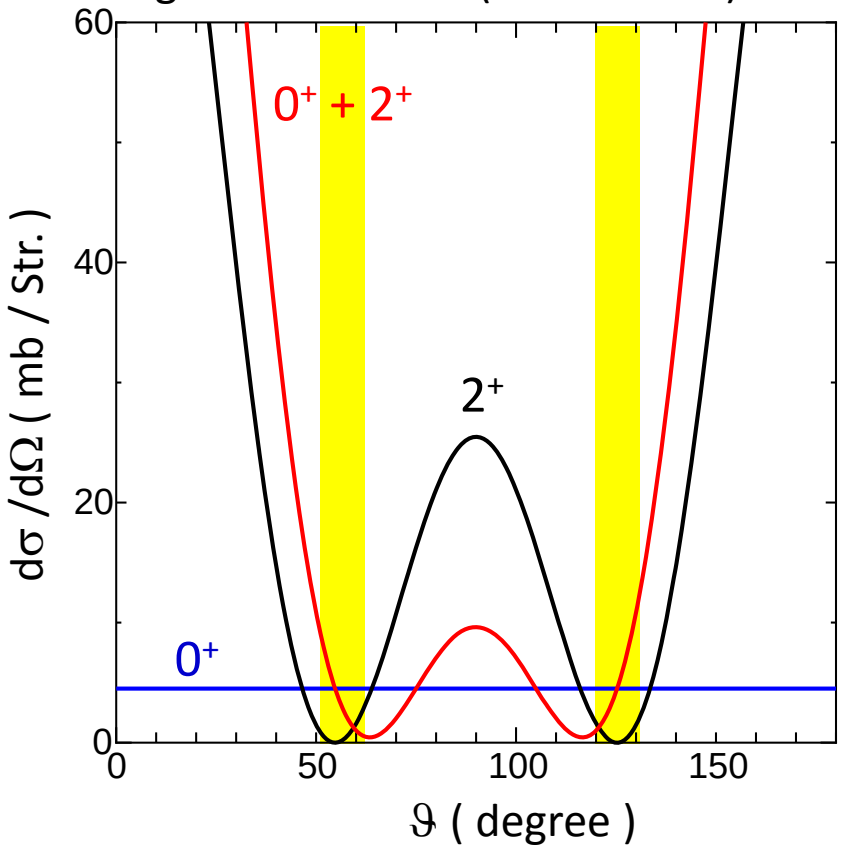

Gate of angular range :

1. ϑ ~ 55 and 125 (degree) ⇒P(J=2)=0

2. 50 < ϑ< 60, 120< ϑ < 130 (degree)

Gating of angular distribution of α+^{8}He ⇒ ^{6}He+^{6}He

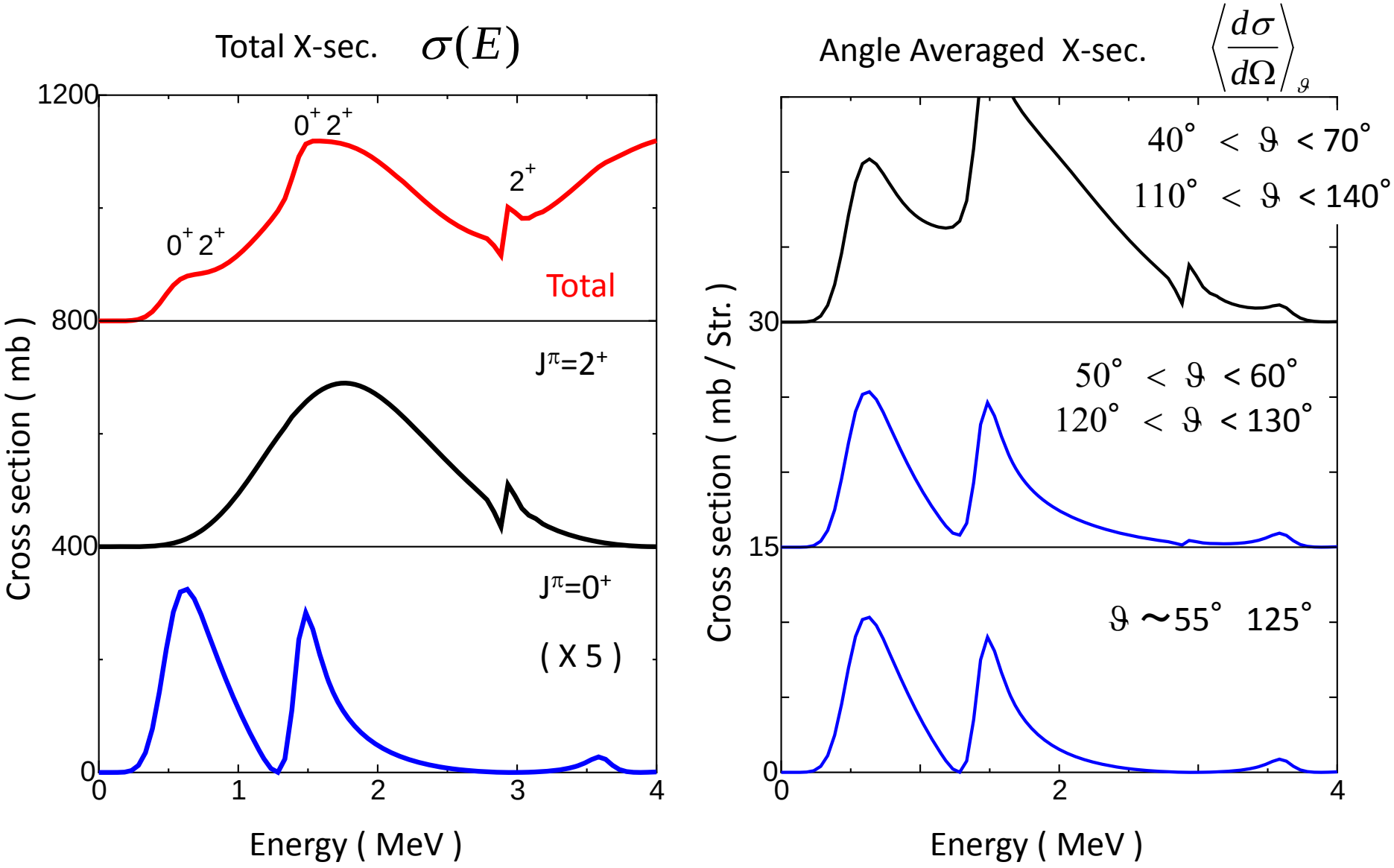

The angle averaged cross section nicely reproduces the 0+ contribution !!

Angular Gate for the non-zero spin states

$\alpha + {}^{8}He \Rightarrow {}^{6}He + {}^{6}He$ (J=2,4,6,8)

J =2 $\vartheta \sim 30^\circ$ 150°

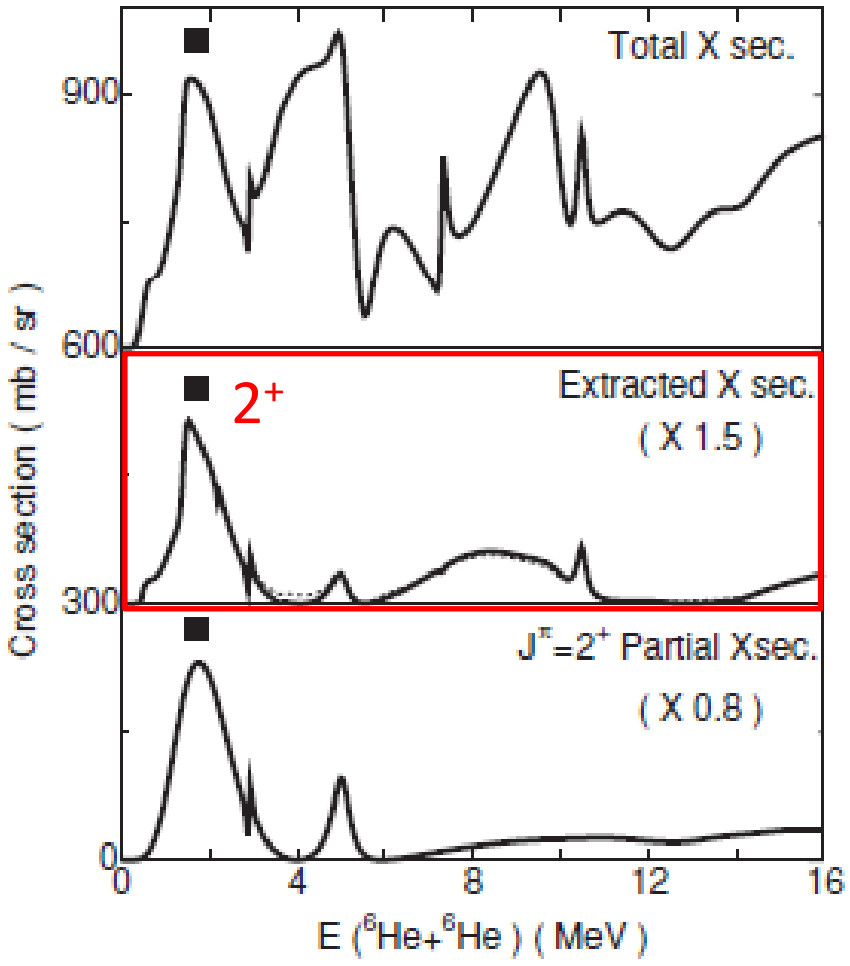

J =4,6,8 $\vartheta = 90^\circ$

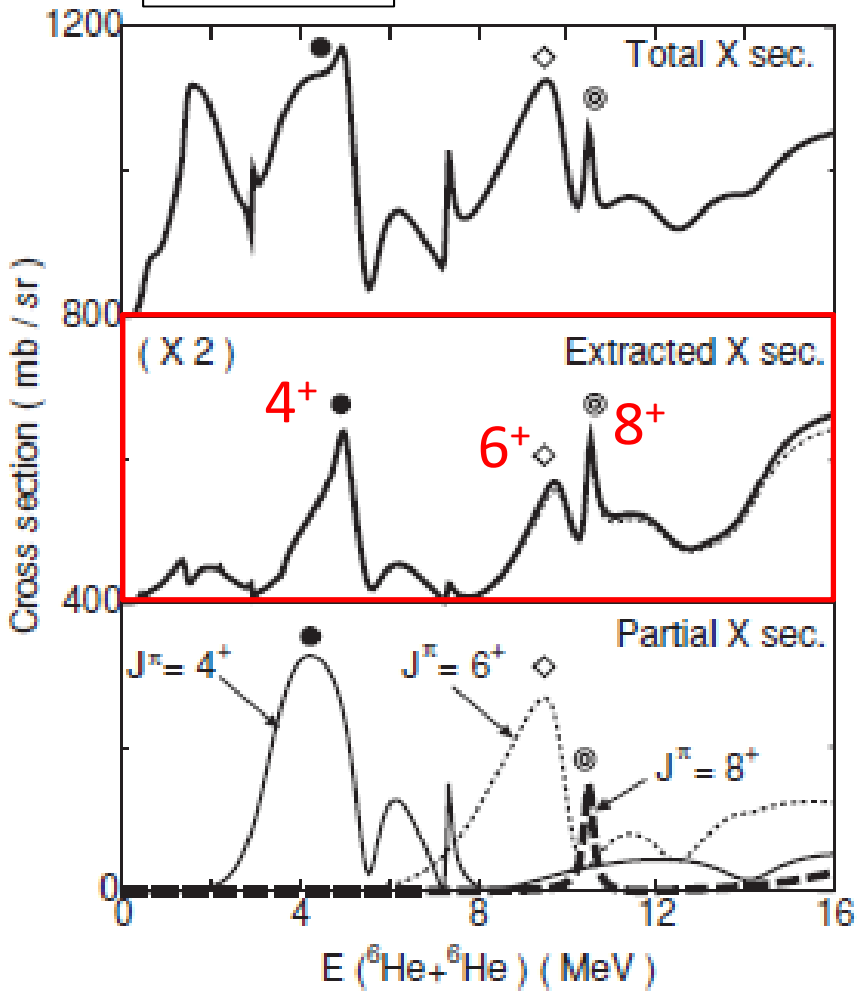

Gate at the 90 degree nicely works for the finite spin of J=4,6,8, but the angular selection should be careful for the low spin states (J=0 and2).

2. モノポール遷移によるクラスター励起

Monopole transition in ^{12}Be : Isoscalar vs Isovector excitations

There is a possibility to identify the excitation degrees of freedom by the combination of the isoscalar and isovector transition

1. Isoscalar monopole transition → responsible to a cluster excitation

$$M(IS) = \left\langle 0_f^+ \left| \sum_{i=1}^{12} r_i^2 \right| 0_1^+ \right\rangle$$

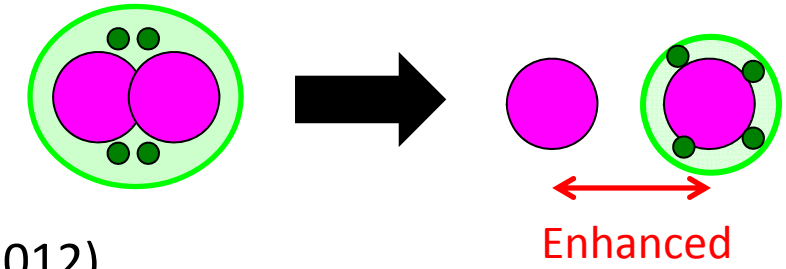

T. Yamada et al., PTP120 (2008); PRC85 (2012)

2. Isovector monopole transition → sensitive to neutron excitations

$$M(IV) = \left\langle 0_f^+ \left| \sum_{i=1}^{12} r_i^2 \tau_{zi} \right| 0_1^+ \right\rangle$$

α−α part is vanished !

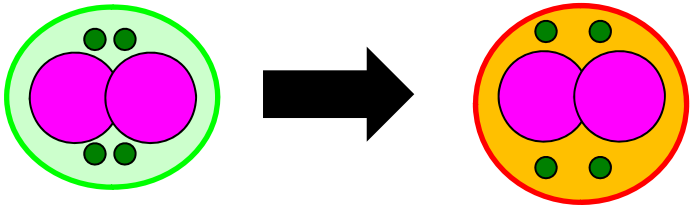

Isoscalar vs Isovector excitations in ^{12}Be

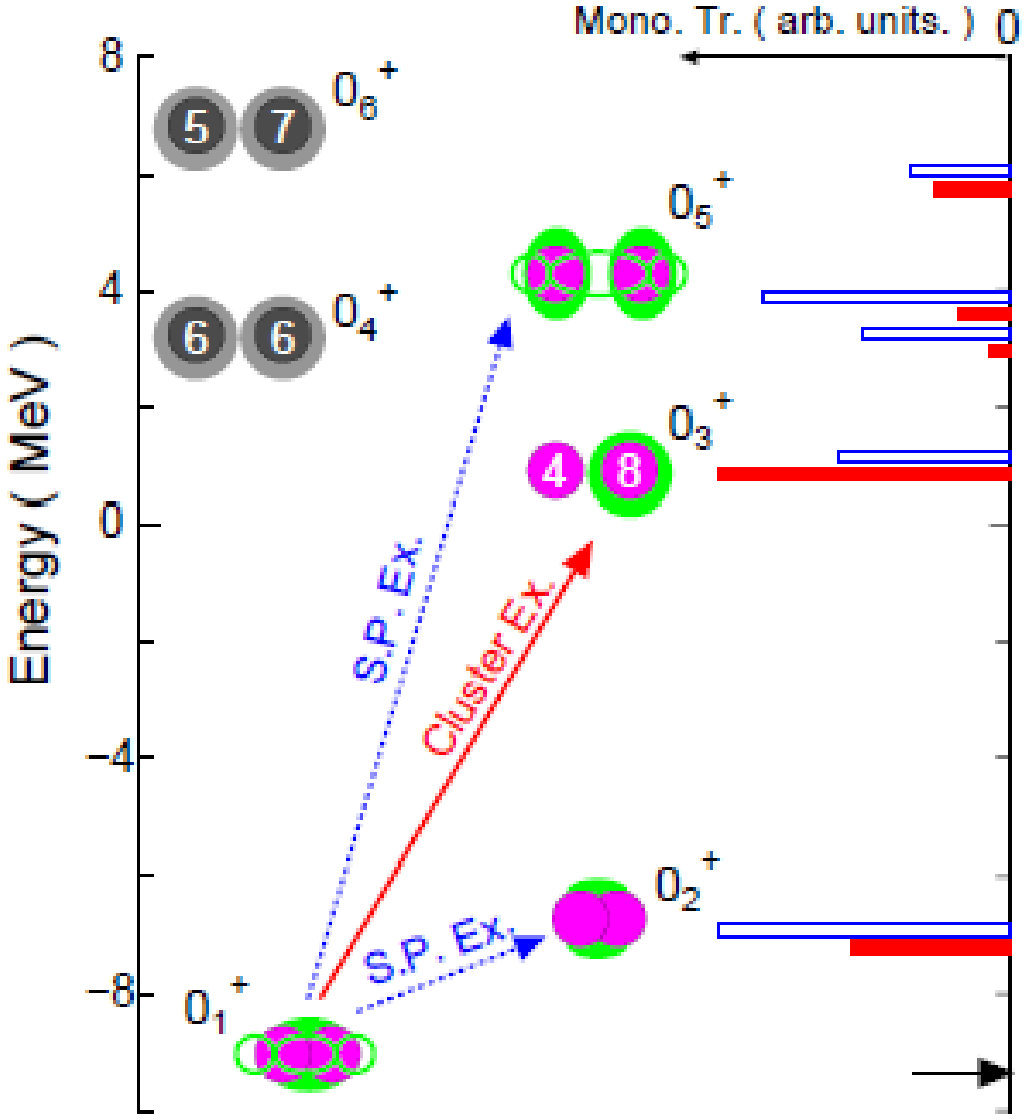

There are clear enhancements in

Isoscalar ⇒ Cluster excitation (0_3^+)

Isovector ⇒ Neutron excitations (0_2^+, 0_5^+)

$$\left|\frac{M(IS,IV)}{M(s.p.)}\right|$$

State	$\lvert\tilde{M}(IS)\rvert$	$\lvert\tilde{M}(IV)\rvert$
0_2^+	2.59	0.98
0_3^+	3.53	0.75
0_4^+	0.92	0.69
0_5^+	1.48	0.90
0_6^+	1.76	0.57

0_3^+ is consistent to the recent exp. by Yang et al., PRL112 (2014)

Monopole strength are comparable to a single particle strength !

^{10}C and ^{10}Be : Mirror symmetry breaking

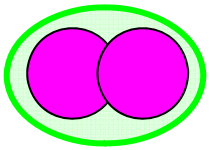

In a recent experiment, there is NO prominent difference in B(E2)↓ between ^{10}Be and ^{10}C

^{10}Be: 9.2 e^2 fm^4 ^{10}C: 8.8 e^2 fm^4

E. A. McCuthan et al., PRC86 (2012)

MO model by N. Itagaki et al. supports the mirror symmetry for ^{10}C and ^{10}Be (RIKEN Accel. Prog. Rep. 36 (2003))

However, the GTCM calculation predicts the prominent difference in the isoscalar monopole transition (M(IS))

	r.m.s. (fm)	$E(0_2^+)$ (MeV) Theory	M(IS) (fm^4) $0_1^+ \Rightarrow 0_2^+$
^{10}Be	2.66	5.03	7.70
^{10}C	2.73	4.00	27.8

M(IS) enhancement in ^{10}C is originated from a kind of Thomas Ehrman shift.

Summary

M. Ito and K. Ikeda, Report on Progress in Physics, 77 096301 (2014)
M. Tomita, M. Iwasaki, R. Otani, and M. Ito, PRC89, 034619 (2014)

We have studied the chemical-bonding cluster structure in Be isotopes, ^{10}C, and ^{18}O. Access to the cluster states by various reactions are also discussed

Results

1. Structure analysis of the light unstable nuclei

① Covalent, ionic and atomic structures appears in excited states

② Wide variety appears by the combination of cluster-core and excess-nucleons

2. Access to the excited states by the reaction

① Resonant scattering is useful to excite the cluster states directly

⇒Characteristic enhancements will be appeared in the branching ratio

② Monopole transition can select the excitation degrees of freedom

⇒IS mono. for the α-α excitation, IV mono. for the neutron excitation

② Scattering radius characterizes a spatial size of the exclusive reaction

⇒Scattering radius is prominently enhanced in the cluster excitation

Unified treatment of the structure and reaction mechanism including the experimental setup is very important

3. 散乱半径法による反応分析

Scattering radius

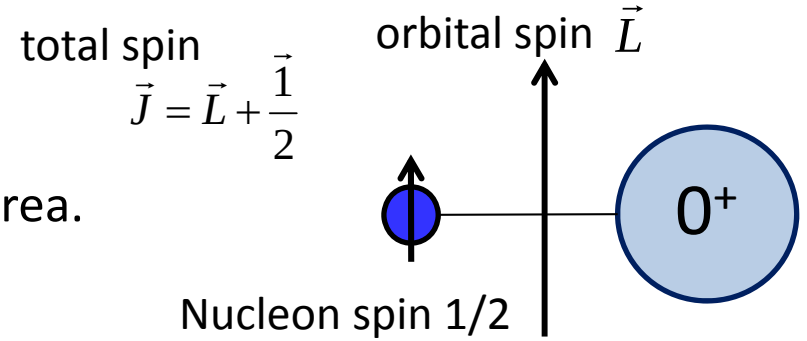

We characterize the spatial size of scattering area.

(1) General scattering theory

$$\left(H(JL) - E\right)\Psi_{JL} = 0 \quad \Rightarrow \text{partial cross section } \sigma(JL)$$

⇒We calculate the radius of the scattering area from $\sigma(JL)$.

(2) Definition of the scattering radius

M. Tomita et al, PRC89 (2014).

Effective orbital spin $\bar{L}$ of an incident wave

$$\bar{L} = \sqrt{\frac{\sum_{JL}\left[\sqrt{L(L+1)}\right]^4 \sigma(JL)}{\sum_{JL}\left[\sqrt{L(L+1)}\right]^2 \sigma(JL)}}$$

$\bar{L} = kR_{SC}$ ⇒ scattering radius: $R_{SC} = \dfrac{\bar{L}}{k}$

cf. mean matter radius

$$\bar{R} = \sqrt{\frac{\int dR R^4 \rho(R)}{\int dR R^2 \rho(R)}}$$

$\rho(R)$:matter density

$\bar{L} = kR_{SC}$ **k, incident wave number**

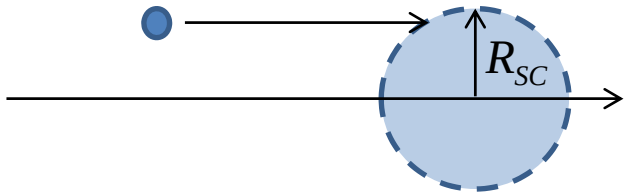

⇒We can always define the scattering radius R_{SC} in the standard scattering calculation.

Scattering radius for channels with a finite spin

For example, we consider the reaction of P + $^{12}C(0_1^+) \Rightarrow p + {}^{12}C^*(S)$

If the final channel has a finite spin S, the partial cross sections are modified like

spinless transition

Initial $0_1^+ \Rightarrow$ Final 0_2^+

$$\sigma(JL)$$

initial and final channels

transition with a finite spin

Initial $0_1^+ \Rightarrow$ Final $2_1^+, 2_2^+, 3_1^-$

$$\sigma(JLL'S)$$

initial ch. final ch. S : final spin

$$\bar{L} = \sqrt{\frac{\sum_{JL}\left[\sqrt{L(L+1)}\right]^4 \sigma(JL)}{\sum_{JL}\left[\sqrt{L(L+1)}\right]^2 \sigma(JL)}} \quad \Rightarrow \quad \bar{L} = \sqrt{\frac{\sum_{JLL'S}\left[\sqrt{L(L+1)}\right]^4 \sigma(JLL'S)}{\sum_{JLL'S}\left[\sqrt{L(L+1)}\right]^2 \sigma(JLL'S)}}$$

L is common in both the initial and final channels

$\bar{L}$ is calculated from the average of the initial orbital spin *L*

Results of the differential cross section

(incident energy E_{lab}=65MeV)

＊ : experimental data

red line : DDM3Y+multi channel

Calculations are done by M. Tomita

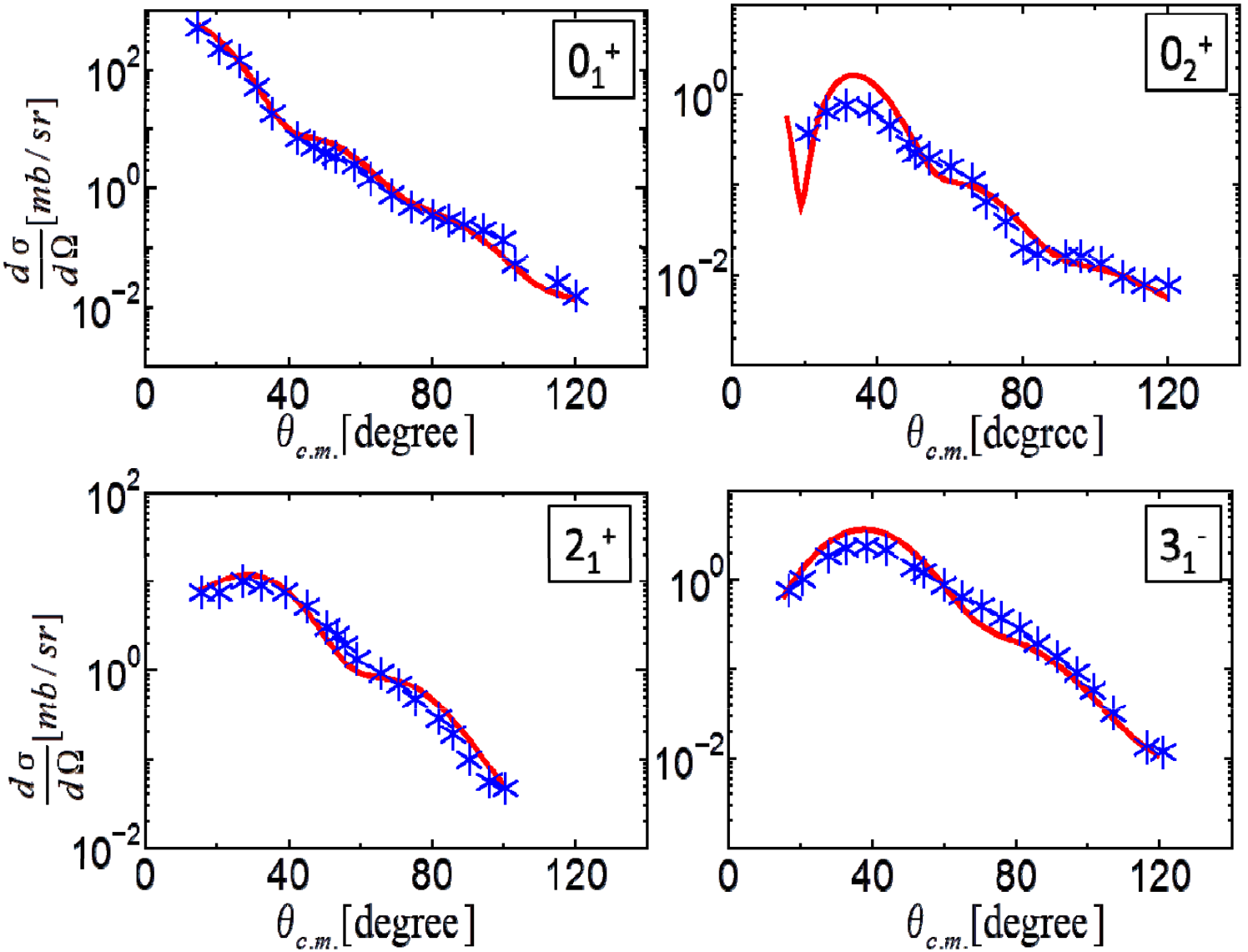

Results of the partial cross section

$$\sigma(J) \leftarrow \sigma(J) / \sum_J \sigma(J)$$

incident energy E_{lab} = 65MeV

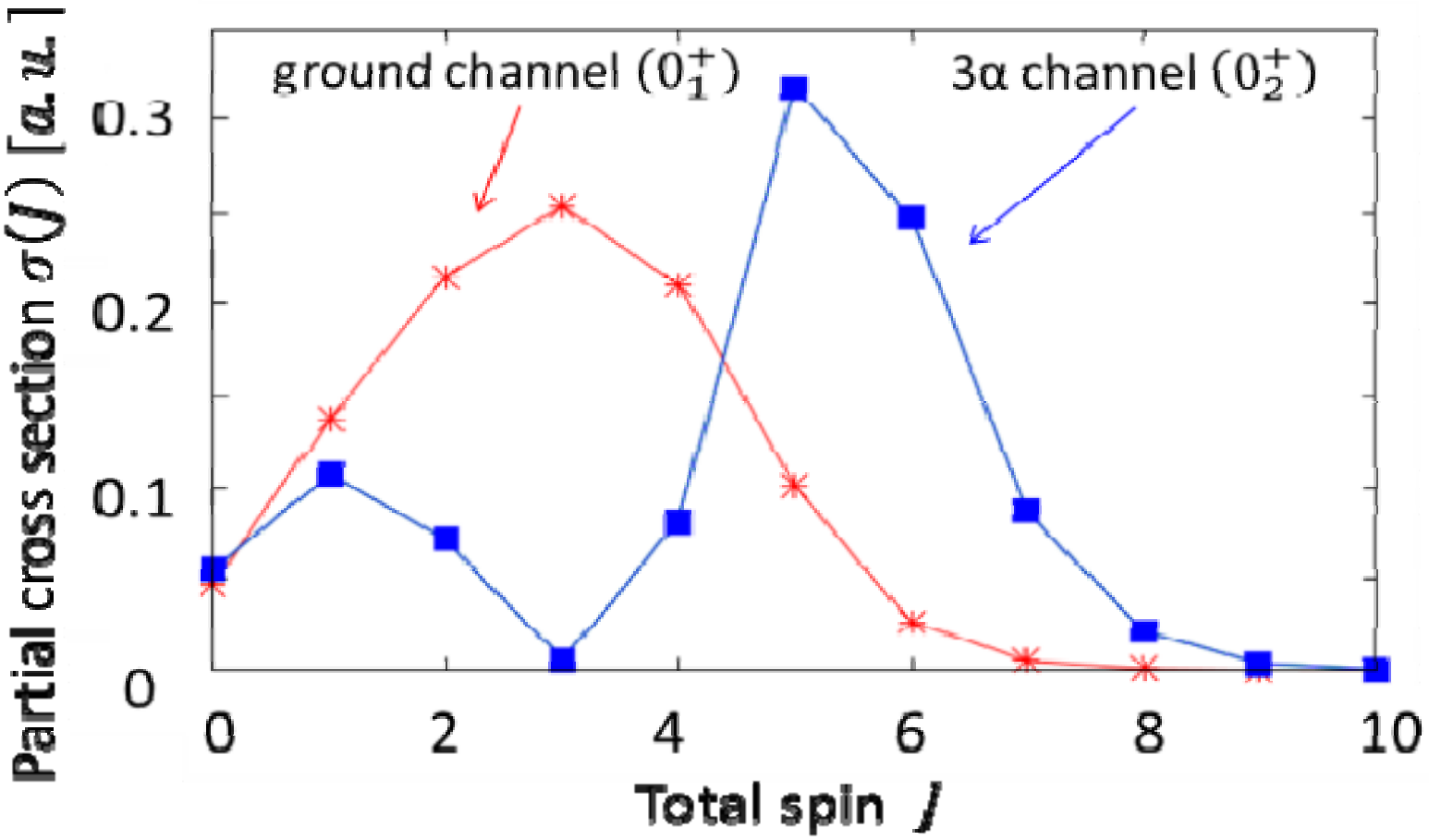

3α channel has the extended distribution

⇒Scattering occurs in the wide spatial region in the 3α channel

Scattering radius with the finite spin

$$\bar{L} = \sqrt{\frac{\sum_{JLL'S}\left[\sqrt{L(L+1)}\right]^4 \sigma(JLL'S)}{\sum_{JLL'S}\left[\sqrt{L(L+1)}\right]^2 \sigma(JLL'S)}} \qquad R_{SC} = \frac{\bar{L}}{k}$$

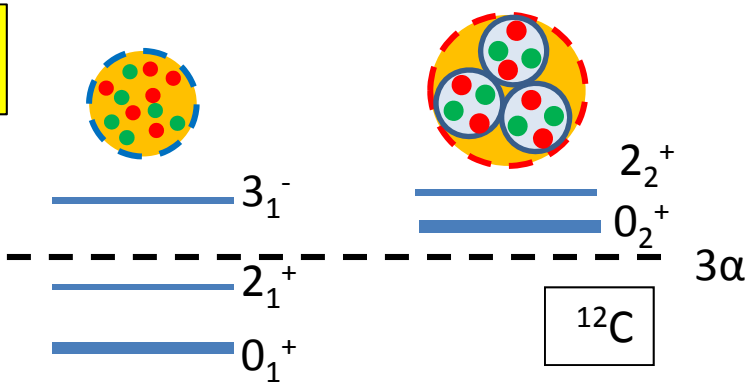

incident energy E_{lab} = 65MeV

	0_1^+	2_1^+	0_2^+	2_2^+	3_1^-
effective orbital spin $\bar{L}$	4.64	5.65	6.37	6.82	5.96
scattering radius Rsc [fm]	2.73	3.32	3.74	4.01	3.51
matter radius $\bar{r}$ [fm]※	2.40	2.38	3.47	4.00	2.76

※M. Kamimura, NPA351 (1981).

Rsc is enhanced in the 0_2^+, 2_2^+ and 3_1^- channels.

The scattering radius of 2_2^+ is strongly enhanced

※Y. Funaki et al., EPJA24 (2005)